

## Unusual Spin State Equilibrium of Azide Metmyoglobin Induced by Ferric Corrphycene

Saburo Neya,<sup>\*,†</sup> Motonari Tsubaki,<sup>‡,§</sup> Hiroshi Hori,<sup>||</sup> Takashi Yonetani,<sup>⊥</sup> and Noriaki Funasaki<sup>†</sup>

Department of Physical Chemistry, Kyoto Pharmaceutical University, Yamashina, Kyoto 607-8414, Japan, Department of Life Science, Faculty of Science, Himeji Institute of Technology, Kamigooori-cho, Akou-gun, Hyogo 678-1297, Japan, Institute for Protein Research, Osaka University, Suita, Osaka 565-0871, Japan, Division of Biophysical Engineering, Graduate School of Engineering Science, Osaka University, Toyonaka, Osaka 560-8531, Japan, and Department of Biochemistry and Biophysics, University of Pennsylvania Medical Center, Philadelphia, Pennsylvania 19104-6089

Received June 22, 2000

Myoglobin was reconstituted with the ferric complex of corrphycene, a novel porphyrin isomer with a rearranged tetrapyrrole array, to investigate the influence of porphyrin deformation on the equilibrium between high-spin ( $S = 5/2$ ) and low-spin ( $S = 1/2$ ) states in the azide derivative. The azide affinity,  $2.5 \times 10^4 \text{ M}^{-1}$ , was 1 order of magnitude lower than the corresponding values of a reference myoglobin containing an electron-deficient diformylheme similar to the corrphycene. Analysis of the visible absorption spectrum over a range of 0–40 °C reveals that the population of high-spin iron is 76–82% at room temperature for azide metmyoglobin complexed with ferric corrphycene. The unusual predominance of the high-spin state was verified from the infrared spectrum of coordinating azide, where the high-spin peak at  $2046 \text{ cm}^{-1}$  is 4-fold larger in intensity than the  $2023 \text{ cm}^{-1}$  low-spin band. Electron paramagnetic resonance at 15 K further indicated that the iron–histidine bond is cleaved to form a five-coordinate derivative in some fraction of the myoglobin. The remarkable high-spin bias of the spin equilibrium at room temperature and cleavage of the iron–histidine bond at 15 K could be explained in terms of the contracted and trapezoidal metallo core that weakens the iron–histidine bond of azide metmyoglobin bearing corrphycene.

## Introduction

Hemoproteins participate in a number of critical biological processes. Biological functions of hemoproteins arise from the integrated molecular framework of porphyrin. The fundamental design of porphyrin, a cyclic tetrapyrrole connected with four bridging carbons, is genetically encoded and invariant over naturally occurring hemes. Rearrangement of the basic skeleton is hardly likely in any metabolic processes of porphyrin. Recent technical advances in the synthesis of porphyrins, however, have enabled us to artificially rearrange the basic framework of porphyrin. One such an analogue is corrphycene, a novel porphyrin isomer independently synthesized in 1994 by Sessler et al.<sup>1</sup> and Aukauloo and Guilard.<sup>2</sup> The macrocycle is formally derived from porphyrin by shifting one *meso* carbon atom into the diagonal *meso* bridge (Figure 1A, inset). The direct pyrrole–pyrrole link and opposite ethene bridge deform the metallo cavity from square to trapezoid.

Corrphycene shares many common properties with porphyrin with respect to the flat structure and capability to chelate various metal ions.<sup>3</sup> The apparent similarities of corrphycene with

porphyrin suggest the possible application of corrphycene to hemoprotein. Owing to the trapezoidal central cavity, corrphycene may serve as a unique tool to perturb the direct vicinity of the iron in hemoprotein. It will be of primary interest to examine the biochemical ability of the curiously shaped porphyrinoid in protein. We have reported a preliminary result that iron corrphycene indeed serves as the prosthetic group of myoglobin (Mb).<sup>4</sup> The corrphycene-substituted ferrous Mb revealed an oxygen affinity that is much lower than that of native Mb. On the other hand, corrphycene-bound metMb still remains to be fully characterized. Since the magnetic properties of the ferric heme moiety is greatly influenced by the iron coordination geometry,<sup>5,6</sup> the spin state of metMb is expected to be susceptible to porphyrin deformation. As for ferric hemes and hemoproteins, four magnetic states are possible; low spin ( $S = 1/2$ ), intermediate spin ( $S = 3/2$ ), high spin ( $S = 5/2$ ), and an equilibrium between the high- and low-spin states.<sup>5,6</sup> The spin state equilibrium of azide hemoprotein is a spectacular example of a subtle balance in the iron coordination geometry. Temperature and pressure affect globin conformation, the  $3d^5$  electronic configuration, and subsequently the spin state equilibrium.<sup>5–9</sup>

\* To whom correspondence should be addressed. E-mail: sneya@mb.kyoto-phu.ac.jp. Fax: +81-75-595-4762.

<sup>†</sup> Kyoto Pharmaceutical University.

<sup>‡</sup> Himeji Institute of Technology.

<sup>§</sup> Institute for Protein Research, Osaka University.

<sup>||</sup> Graduate School of Engineering Science, Osaka University.

<sup>⊥</sup> University of Pennsylvania Medical Center.

(1) Sessler, J. L.; Brucker, E. A.; Weghorn, S. J.; Kisters, M.; Schäfer, M.; Lex, J.; Vogel, E. *Angew. Chem., Int. Ed. Engl.* **1994**, *33*, 2308–2312.

(2) Aukauloo, M. A.; Guilard, R. *New J. Chem.* **1994**, *18*, 1205–1207.

(3) Sessler, J. L.; Gebauer, E.; Vogel, E. In *The Porphyrin Handbook*; Kadish, K. M., Smith, K. M., Guilard, R., Eds.; Academic Press: New York, 2000; Vol. 2, pp 1–54.

(4) Neya, S.; Funasaki, N.; Hori, H.; Imai, K.; Nagatomo, S.; Iwase, T.; Yonetani, T. *Chem. Lett.* **1999**, 989–990.

(5) Iizuka, T.; Yonetani, T. *Adv. Biophys.* **1970**, *1*, 157–182.

(6) Scheidt, W. R.; Reed, C. A. *Chem. Rev.* **1981**, *81*, 543–555.

(7) Neya, S.; Hada, S.; Funasaki, N. *Biochim. Biophys. Acta* **1985**, *828*, 241–246.

(8) Neya, S.; Hada, S.; Funasaki, N.; Umemura, J.; Takenaka, T. *Biochim. Biophys. Acta* **1985**, *827*, 157–163.

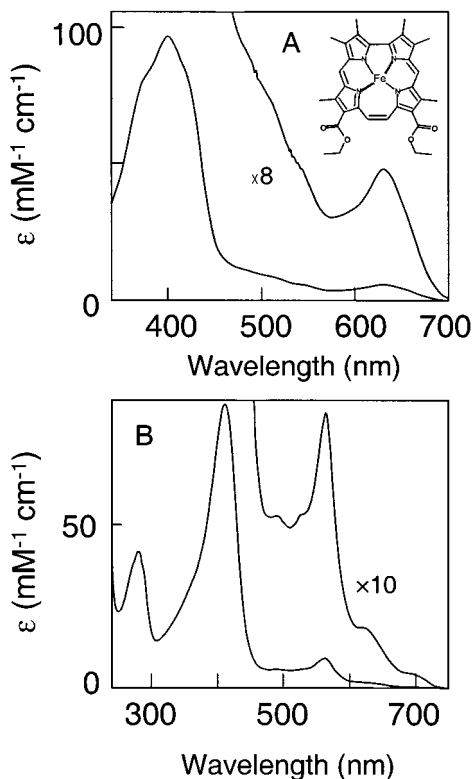


**Figure 1.** Electronic absorption spectra: (A) ferric corrphycene chloride in chloroform at 20 °C (inset: structure of the corrphycene); (B) Mb reconstituted with the ferric corrphycene in 0.1 M Tris at pH 7.0 and 20 °C. The Soret peak is 2.20-fold higher than the 280 nm globin band.

It is very likely that the equilibrium balance is also modulated by the skeletal rearrangement of the porphyrin macrocycle, although such an influence has not been so far evaluated. We report here the first examination on the spin state of azide metMb reconstituted with corrphycene.

### Experimental Section

**Prosthetic Group.** The corrphycene with diethoxycarbonyl groups was used throughout the investigation. It was synthesized according to the method of Neya et al.<sup>10</sup> and iron was inserted following the procedure of Adler et al.<sup>11</sup> The resultant ferrous corrphycene was oxidized in the presence of air before purification by chromatography on a silica gel column (chloroform–methanol (95/5 v/v)). Five-coordinate ferric corrphycene azide was derived from the  $\mu$ -oxo dimer by acid cleavage with dilute aqueous perchloric acid containing a saturating amount of sodium azide. The  $pK_3$  value, which reflects the third protonation at the central pyrrole nitrogen atoms in neutral corrphycene free base, was determined according to the method used for octaethylporphyrin.<sup>12</sup> Briefly, corrphycene dissolved in sulfuric acid was diluted with 2.5% aqueous sodium lauryl sulfate at 20 °C, adjusted to pH 7 with aqueous sodium hydroxide, and titrated back with small increments of hydrochloric acid to pH 2. The Soret spectral changes were analyzed with the Henderson–Hasselbach equation,  $\text{pH} = \text{p}K_3 + \log([\text{neutral form}]/[\text{acid form}])$ .

**Protein Reconstitution.** Sperm whale Mb was available from Sigma (type II). The Mb reconstitution with ferric corrphycene was carried

out by following the method for the octamethylheme-substituted Mb.<sup>13</sup> The crude protein was purified by column chromatography on a carboxymethylated cellulose column (Whatman, CM52) using a linear gradient elution with Tris buffer (20–120 mM) at pH 7.0 and 4 °C. The main fractions with  $A_{\text{Soret}}/A_{280} > 2.20$  were collected. The typical reconstitution yield was 50–60%. The extinction coefficient of purified metMb was determined to  $\epsilon_{411 \text{ nm}} = 87 \text{ mM}^{-1} \text{ cm}^{-1}$  on the basis of the pyridine hemochromogen spectrum of the ferric corrphycene. The hemochromogen spectrum, exhibiting  $\lambda_{\text{max}}$  (nm) ( $\epsilon$ ,  $\text{mM}^{-1} \text{ cm}^{-1}$ ) at 421 (126), 495 (12.9), 542 (14.7), and 561 (19.3), was recorded immediately after addition of a small amount of reducing agent, aqueous sodium dithionite, to the ferric corrphycene in pyridine–dimethylformamide (1/1 v/v).

**Physical Measurements.** Ligand binding constants were spectrophotometrically determined on a Shimadzu MPS-2000 spectrophotometer with a thermostated sample holder. Electron paramagnetic resonance (EPR) at X-band (9.35 GHz) was measured with a Varian E-12 spectrometer with 100 kHz field modulation (0.5 mT). A cryostat (Oxford, ESR-900) was used for observation at 15 K. Infrared (IR) spectra were recorded at 4  $\text{cm}^{-1}$  resolution using a  $\text{CaF}_2$  cell of 50  $\mu\text{m}$  path length on a Perkin-Elmer Model 1850 Fourier transform IR spectrophotometer. A less than stoichiometric amount of sodium azide was added to corrphycene metMb to minimize the band of the free azide. The IR absorption spectra in the 1900–2100  $\text{cm}^{-1}$  region were obtained from the difference between azide metMb and the buffer solution. An average of 200 scans was used for each spectrum. In the measurements of thermochromism, the temperature of the Mb solution was monitored with a precision thermometer (YSI, Model 4610) equipped with a probe dipped into the cuvette.

### Results

**Prosthetic Group and Reconstituted Myoglobin.** The free base of corrphycene is known to have a porphyrin-like absorption with an intense 416 nm Soret band.<sup>10</sup> The ferric chloride complex shows an absorption spectrum with peaks at 399 (Soret) and 630 nm and weak shoulders around 370, 420, 490, 510, and 540 nm (Figure 1A). The  $pK_3$  value ( $=2.4 \pm 0.2$ ) for the free base corrphycene is significantly lower than the  $pK_3$  value ( $=4.8$ ) for protoporphyrin.<sup>14</sup>

The reconstituted metMb exhibits a characteristic light absorption profile. In the visible region, a single dominant peak at 562 nm is accompanied by four weak absorptions at 495, 530, 620, and 700 nm (Figure 1B). The Soret band at 411 nm is only 2.20-fold larger than the protein peak at 280 nm. This result is reproducible, and further purification of the Mb did not improve this ratio.

The visible absorption of corrphycene metMb is remarkably pH-dependent. The Soret peak was reversibly suppressed with increasing pH from 7 to 9 with isosbestic points at 362 and 428 nm (Figure 2). Analysis of the changes in the absorbance at 415 nm revealed a transition associated with a single proton equilibrium with  $pK_a = 7.87 \pm 0.21$ , being consistent with an equilibrium of association/dissociation of a single proton. The behavior, similar to the acid–alkaline transition of native Mb,<sup>15</sup> suggests the presence of a bound water molecule as the sixth iron ligand. Several anionic and neutral ligands coordinate to the metMb. The ligand affinities of  $\text{CN}^-$ ,  $\text{SCN}^-$ ,  $\text{OCN}^-$ , and  $\text{F}^-$  were  $3.1 \times 10^5$ ,  $3.3 \times 10^3$ ,  $1.3 \times 10^3$ , and  $1.6 \times 10^2 \text{ M}^{-1}$ , respectively. These values, except for  $\text{CN}^-$ , are comparable to those reported for diformylheme Mb.<sup>15</sup> The visible spectra of

(9) Messana, C.; Cerdonio, M.; Shenkin, P.; Noble, R. W.; Fermi, G.; Perutz, R. N.; Perutz, M. F. *Biochemistry* **1978**, *17*, 3652–3662.  
 (10) Neya, S.; Nishinaga, K.; Ohya, K.; Funasaki, N. *Tetrahedron Lett.* **1998**, *39*, 5217–5220.  
 (11) Adler, A. D.; Longo, F. R.; Kampas, F.; Kim, J. *J. Inorg. Nucl. Chem.* **1970**, *32*, 2443–2445.  
 (12) Neya, S.; Funasaki, N.; Imai, K. *J. Biol. Chem.* **1988**, *263*, 8810–8815.

(13) Neya, S.; Funasaki, N.; Shiro, Y.; Iizuka, T.; Imai, K. *Biochim. Biophys. Acta* **1994**, *1208*, 31–37.  
 (14) Caughey, W. S. In *Inorganic Biochemistry*; Eichhorn, G. L., Ed.; Elsevier: New York, 1973; Vol. 2, pp 797–831.  
 (15) Sono, M.; Asakura, T. *J. Biol. Chem.* **1976**, *251*, 2664–2670.

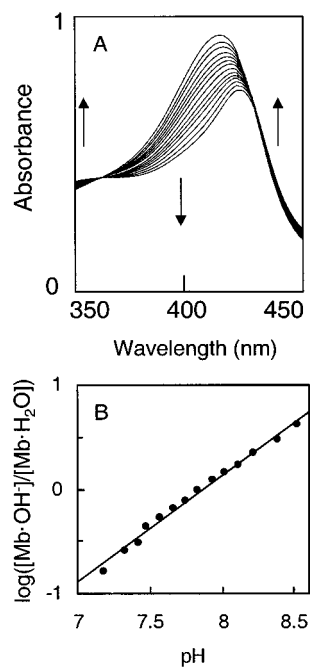


**Figure 2.** Acid-alkaline transition of corrrhycene-substituted metMb: (A) pH-dependent Soret spectra in 5 mM Tris at 20 °C, with the pH increasing from 7.18 to 7.32, 7.42, 7.47, 7.56, 7.66, 7.66, 7.74, 7.83, 7.93, 8.01, 8.11, 8.21, 8.38, and 8.52 as indicated by the arrows and with isosbestic points at 362 and 428 nm; (B) analysis of the spectral changes at 415 nm with  $pK_a = 7.87 \pm 0.07$ .

**Table 1.** Visible Absorption of the Metmyoglobin Derivatives Reconstituted with Corrrhycene in 0.1 M Tris at pH 7.0 and 20 °C

ligand	$\lambda_{max}$ , nm ( $\epsilon$ , $\text{mM}^{-1} \text{cm}^{-1}$ )					
H <sub>2</sub> O	411 (87)	490 (6.5)	525 (6.3)	562 (9.1)	620 (2.4)	700 (0.5)
CN <sup>-</sup>	418 (97)	490 (7.9)		569 (6.8)		700 (0.5)
OCN <sup>-</sup>	416 (76)	495 (6.2)	530 (6.5)	564 (9.5)	621 (2.4)	690 (0.9)
SCN <sup>-</sup>	417 (88)	500 (7.8)	533 (7.5)	569 (10.2)	630 (2.0)	700 (0.8)
N <sub>3</sub> <sup>-</sup>	422 (76)	500 (7.6)	530 (7.8)	562 (9.4)	625 (2.5)	680 (1.1)
F <sup>-</sup>	422 (86)	490 (9.0)		553 (8.4)	630 (3.8)	

the metMb derivatives are summarized in Table 1. The spectra with a dominant band near 560 nm are quite distinguishing.

**Thermal Spin State Equilibrium.** Corrrhycene metMb binds with azide ion as well (Figure 3), although the association constant  $2.5 \times 10^4 \text{ M}^{-1}$  is 1 order of magnitude lower than the corresponding value of  $4.0 \times 10^5 \text{ M}^{-1}$  reported for diformylheme metMb.<sup>15</sup> The azide complex displays obvious thermochromism, a visible absorption change associated with temperature, as indicated in Figure 4A. With increasing temperature over a 0–40 °C range, the absorbance reversibly increased at 580 nm and decreased at 560 nm with well-defined isosbestic points at 568 and 613 nm. These isosbestic points are different from those found during azide titration to the aquo metMb and suggest a thermal transition between the two states. We assigned this phenomenon to the equilibrium between the high-spin ( $S = 5/2$ ) and low-spin ( $S = 1/2$ ) states with the latter being as ground state, as has been extensively reported for a number of N<sub>3</sub><sup>-</sup> hemes<sup>6,8,16,17</sup> and hemoproteins.<sup>5,8,9,18</sup> Analysis of the thermochromism, according to the reported procedures,<sup>7</sup> afforded  $\Delta H = -2990 \pm 70 \text{ cal/mol}$ ,  $\Delta S = -13.3 \pm 0.3 \text{ eu}$ , and the midpoint of transition at  $225 \pm 12 \text{ K}$  (Figure 4B). The

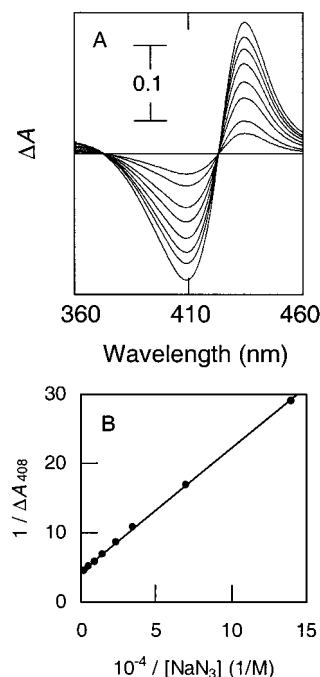


**Figure 3.** Azide titration to corrrhycene metMb: (A) Soret difference spectra induced by sodium azide in 0.1 M Tris at pH 7.0 and 20 °C, with an Mb concentration is 13  $\mu\text{M}$  and the azide concentration increasing from 0 to 7.2, 14.3, 28.7, 43.0, 71.6, 115, 186, and 472  $\mu\text{M}$ ; (B) analysis of the 408 nm transition. The binding constant is  $(2.48 \pm 0.17) \times 10^4 \text{ M}^{-1}$ .

estimated high-spin fraction,  $0.82 \pm 0.04$  at 20 °C, is remarkably larger than the 0.05–0.10 reported for other azide hemoprotein derivatives under comparable conditions.<sup>6–9,17–20</sup>

**Infrared Measurements.** We examined the IR spectrum of the coordinating N<sub>3</sub><sup>-</sup> in an attempt to evaluate the analysis with thermochromism. Figure 5 shows the IR spectra for the azide internal antisymmetric stretching region of the metMb. Two main bands appeared at 2046 and 2024  $\text{cm}^{-1}$  with a bandwidth of 12–14  $\text{cm}^{-1}$ . The spectra were recorded in the presence of only a half-saturating amount of sodium azide to minimize the contribution from the free N<sub>3</sub><sup>-</sup>, which produced a broad band at 2049  $\text{cm}^{-1}$  with a half-bandwidth of 26  $\text{cm}^{-1}$ . The two stretching bands at 2046 and 2024  $\text{cm}^{-1}$  are identical with those at 2046 and 2024  $\text{cm}^{-1}$  found in other native and mutant Mbs with protoheme.<sup>19,20</sup> The 2046 and 2024  $\text{cm}^{-1}$  peaks are unambiguously derived from the coordinating N<sub>3</sub><sup>-</sup>, because the terminal <sup>15</sup>N label in N<sub>3</sub><sup>-</sup> splits them into four new bands at 2041, 2027, 2014, and 2005  $\text{cm}^{-1}$  (results not shown) due to the end-on coordination. The separation of each N<sub>3</sub><sup>-</sup> IR species, i.e., 14 and 9  $\text{cm}^{-1}$ , respectively, is also comparable to those for native Mb and hemoglobin (results not shown). The appearance of the two bands indicates the coexistence of the two spin states, as suggested from thermochromism in Figure 4. We assigned the band at 2046  $\text{cm}^{-1}$  to high-spin species and the 2024  $\text{cm}^{-1}$  signals to the low-spin form from comparison of the result with that for the native Mb.<sup>19</sup> Consistent with this assignment, the low-spin band at 2024  $\text{cm}^{-1}$  was slightly intensified at 2 °C relative to the 2024  $\text{cm}^{-1}$  band. The IR spectra in Figure 5 exhibit a prominent profile in which the high-spin band at 2046  $\text{cm}^{-1}$  is the major component. This is in remarkable contrast with the reported IR observation for most

(16) Huang, Y.-P.; Kassner, R. J. *J. Am. Chem. Soc.* **1979**, *101*, 5807–5810.

(17) Zhang, Y.; Hallows, W. A.; Ryan, W. J.; Jones, J. G.; Carpenter, G. B.; Sweigart, D. A. *Inorg. Chem.* **1994**, *33*, 3306–3312.

(18) Neya, S.; Funasaki, N. *Biochemistry* **1986**, *25*, 1221–1226.

(19) Alben, J. O.; Fager, L. Y. *Biochemistry* **1972**, *11*, 842–847.

(20) Bogmil, R.; Hunter, C. L.; Maurus, R.; Tang, H.-L.; Lee, H.; Lloyd, E.; Brayer, G.; Smith, D. M.; Mauk, A. G. *Biochemistry* **1994**, *33*, 7600–7608.

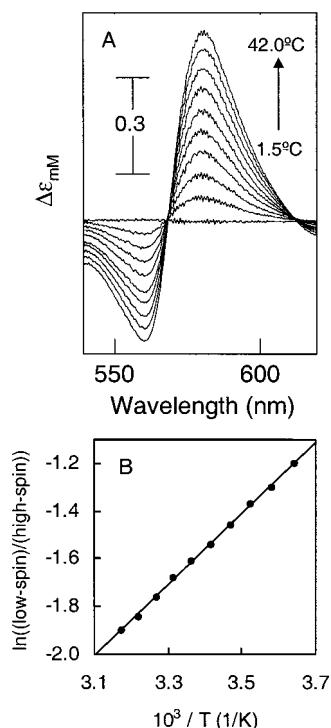


**Figure 4.** Thermochromism of azide metMb bearing corrphycene: (A) changes in the 540–620 nm region with increasing temperature from 1.48 to 60.1, 10.52, 14.98, 19.45, 24.06, 28.49, 32.98, 37.50 and 41.98 °C (protein concentration 116  $\mu\text{M}$  in 0.1 M Tris, pH 7.0, containing 0.1 M sodium azide); (B) van't Hoff plots from the 580 nm changes, corresponding to  $\Delta H = -2990 \pm 70$  cal/mol and  $\Delta S = -13.3 \pm 0.3$  eu.

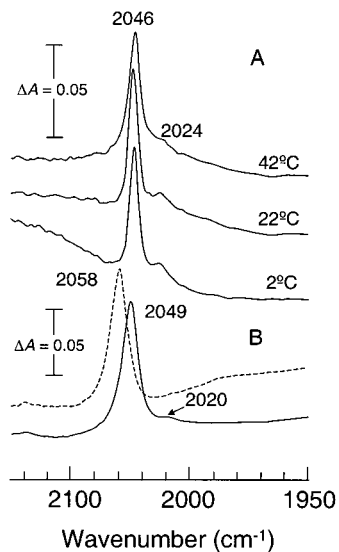


**Figure 5.** IR absorption spectra of azide stretching bands for metMb and model compounds: (A) temperature-dependent corrphycene azide metMb (protein concentration 1 mM and azide concentration 0.5 mM in 0.1 M Tris at pH 7.0); (B) model complexes in chloroform at 20 °C, showing the five-coordinate ferric corrphycene azide (broken line) and six-coordinate ferric corrphycene azide/1-methylimidazole (solid line, [1-methylimidazole] = 1 mM).

azide complexes of metMb,<sup>19,20</sup> for which the high-spin peak at 2046  $\text{cm}^{-1}$  is a minor component. At room temperature, the intensity ratio of the two bands is  $I_{2046}/I_{2024} = 4.0$  in Figure 5. The intensity ratio parallels the high-spin fraction 0.82 at 20 °C, as estimated from thermochromism in Figure 4. An additional feature in Figure 5 is the minor temperature dependence of the IR spectra. This is also in agreement with the small

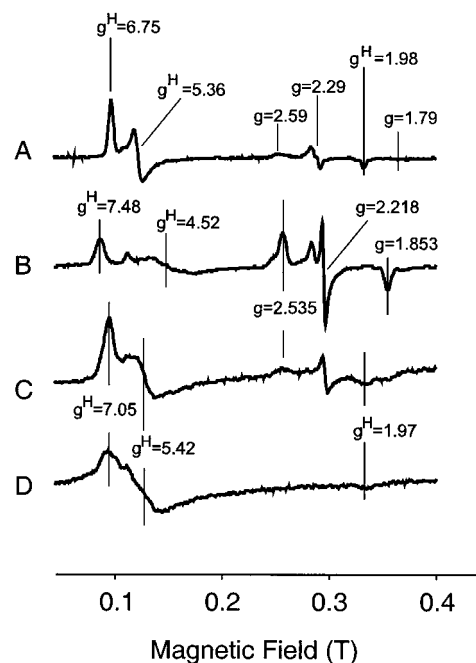


**Figure 6.** EPR spectra of the corrphycene complexes at 15 K: (A) aquo metMb in 0.1 M Tris at pH 7.0; (B) azide metMb at in 0.1 M Tris at pH 7.0; (C) azide metMb at in 0.1 M phosphate at pH 7.0; (D) five-coordinate ferric corrphycene azide in chloroform.  $g^H$  denotes the  $g$  value for the high-spin component.

changes in the low-spin populations, 0.21 at 0 °C and 0.14 at 40 °C, as estimated from Figure 4. Thus, the observations with IR spectra are fully consistent with the results from the thermochromism and suggest a low-spin ground state for the equilibrium. In Figure 5, IR spectra of model compounds, a five-coordinate ferric corrphycene azide and the six-coordinate azide/1-methylimidazole derivative in chloroform, are also provided. The IR spectrum of the mixed-ligand model complex closely resembles the protein spectrum. The position of the high-spin bands in the six-coordinate model is different from that of the five-coordinate compound, indicating that the high-spin component of the model azide/1-methylimidazole complex does not come from the dissociation of the iron-bound 1-methylimidazole.

**Electron Paramagnetic Resonance.** We recorded the EPR spectrum at 15 K to further examine the azide complex of corrphycene Mb. Figure 6A illustrates the aquo metMb spectrum, where the high-spin signal around  $g = 6$  splits into two peaks due to lower symmetry of the prosthetic group. The minor low-spin component with  $g = 2.59, 2.29,$  and  $1.79$  may reflect the partial ligation of the distal histidine. The azide complex in Figure 6B shows a rhombic high-spin signal with  $g = 7.5$  and  $4.5$  as well as the low-spin component at  $g = 2.54, 2.22,$  and  $1.85$ . Appearance of the high-spin component is quite unexpected, because the thermodynamic parameters from the thermochromism (Figure 4) indicate a high-spin fraction of less than  $1.0 \times 10^{-6}$  at 15 K. The high-spin signals of the azide complex depend on the buffer. In phosphate, the high-spin  $g$  values were observed at 7.1, 5.4, and 1.97 (Figure 6C). It is also notable that the high-spin signals of azide metMb in phosphate buffer (Figure 6C) closely resemble those of five-coordinate azide corrphycene in chloroform (Figure 6D).

## Discussion

**Structural Integrity and Visible Spectra of Corrphycene Myoglobin.** The attempted alkaline hydrolysis of the ester



groups attached to the corrphycene periphery in a refluxing aqueous alkaline medium intensively decomposed the macrocycle. This is consistent with the theoretical prediction that corrphycene, despite the presence of 18- $\pi$ -electron conjugation, is less stable than porphyrin.<sup>21</sup> Mb reconstitution was thus carried out with the corrphycene bearing two carboxylic ester groups. Since apoMb is known to accommodate all-alkyl hemes,<sup>12,13</sup> it is not surprising that the corrphycene without free carboxyl groups was successfully introduced into the heme pocket. The resultant protein is a stable aquo metMb (Figure 2). Coordination of an iron-bound water molecule and the reversible oxygen binding of the ferrous complex<sup>4</sup> suggest structural integrity of the Mb with a corrphycene prosthetic group. The absorption spectra in Table 1 are dissimilar to any known spectra of Mb.<sup>15,22</sup> For native metMb, an empirical correlation between Soret peak positions and the spin state of ferric iron, i.e., the longer wavelength is associated with the lower spin, has been proposed.<sup>22</sup> The Soret maxima of CN<sup>-</sup> (418 nm), F<sup>-</sup> (422 nm), and other derivatives in Table 1 indicate that such a relationship does not hold any more after core rearrangement of porphyrin into corrphycene.

**Influence of Ester Side Chains.** Strongly electron-withdrawing ester groups on the periphery are expected to lower the electron density over the macrocycle. The  $pK_3$  value is diagnostic of the electronic influence.<sup>14,15</sup> It is notable that  $pK_3 = 2.4$  for the corrphycene is significantly smaller than  $pK_3 = 4.8$  for protoporphyrin<sup>15</sup> to manifest an inductive effect of the ester side chains. The influence subsequently comes up to the central iron atom to facilitate dissociation of the coordinating water molecule into hydroxide anion. The  $pK_a = 7.9$  of the acid-alkaline transition in aquo metMb is expectedly lower than  $pK_a = 8.7$  for native Mb.<sup>15</sup> The ester groups control the ligand binding as well. Corrphycene metMb, owing to increased positive charge on the ferric iron, exhibits higher affinities for ionic ligands such as SCN<sup>-</sup>, OCN<sup>-</sup>, and F<sup>-</sup> as compared with native protein.<sup>15</sup> Thus, corrphycene Mb resembles the metMb having electronegative diformylheme<sup>15</sup> in the two profiles of acid-alkaline transition and ligand binding.

**Unique Aspect of Spin State Equilibrium.** According to Sono and Asakura,<sup>15</sup> the formyl groups enhance the affinity for anionic N<sub>3</sub><sup>-</sup> and the charge attraction of the coordinating N<sub>3</sub><sup>-</sup>, thereby shifting spin equilibrium toward low spin. Thus, it is reasonable to expect a similar high binding affinity for N<sub>3</sub><sup>-</sup> and shift in spin equilibrium to the low spin for corrphycene metMb bearing electronegative ester groups. In contrast to this expectation, the N<sub>3</sub><sup>-</sup> affinity for corrphycene metMb is lowered as compared with diformylheme metMb.<sup>15</sup> The binding constant  $2.5 \times 10^4 \text{ M}^{-1}$  is only  $1/16$  of  $4.0 \times 10^5 \text{ M}^{-1}$  for diformylheme metMb. The depressed N<sub>3</sub><sup>-</sup> affinity suggests some coordination anomaly. The spin equilibrium profile is accordingly irregular. Thermochromism in Figure 4A indicates that the azide complex is predominantly in the high-spin state. This result is not only contrary to the expectation from the inductive effect of the ester groups but is also in remarkable contrast to native azide metMb, which is exclusively low spin.<sup>7,9,18-20</sup> The IR analysis in Figure 5 further indicates that the high-spin species observed at room temperature is not from five-coordinate azide corrphycene. The IR spectra of corrphycene Mb is reminiscent of the IR result of carp azide hemoglobin in the T state.<sup>23</sup> The quantitative analysis

of the thermochromism (Figure 4B) provides an estimated 78–86% population of the high-spin state at room temperature. The remarkable increase in high-spin content may be primarily related to an anomaly in the coordination structure of corrphycene with distinguishing molecular shape. According to the X-ray analysis,<sup>1,3</sup> the metallo cavity of corrphycene, 8.273 Å<sup>2</sup>, is narrower than the 8.503 Å<sup>2</sup> cavity of porphyrin. The contracted core shortens the iron-pyrrole bonds. The shorter equatorial bonds in turn cause the longer axial bonds. Such a correlation between equatorial and axial bond lengths has been established after intensive X-ray studies on ferric azide porphyrins in spin equilibrium.<sup>6,17</sup> In terms of coordination chemistry, the weaker the axial field, the smaller the 3d orbital splitting of ferric iron and the more likely the existence of a high-spin state. We propose that the narrower metallo cavity which modulates modestly the axial ligand field is a main contributing factor for the equilibrium shift to the high-spin state for the azide metMb.

Corrphycene has another structural account that favors the high-spin state. The trapezoidal metallo core results in iron-pyrrole linkages with longer and shorter bond distances.<sup>3</sup> The nonequivalent equatorial bonds could destabilize the in-plane configuration of the iron atom, tending to extrude it out of the corrphycene plane, and favoring the high-spin state. Since azide ion is a stronger axial ligand than imidazole,<sup>8</sup> the iron atom is very likely to be displaced toward azide ion, as has been demonstrated in the model hemin with mixed ligands of N<sub>3</sub><sup>-</sup> and 1-methylimidazole.<sup>17</sup> It is notable in Figure 6 that the  $g$  values of the high-spin EPR signal of azide Mb (Figure 6B,C) are distinct from those of the aquo metMb (Figure 6A). This precludes partial azide dissociation from the Mb. Dissolution of the frozen EPR sample reproduced the visible spectrum before freezing, suggesting that separation of the iron corrphycene from the heme pocket is also unlikely. The most probable origin of the high-spin signals for azide metMb (Figure 6B,C) is the partial rupture of the iron-histidine bond induced by globin conformational change upon sample freezing. The freezing-induced rupture of the iron-histidine bond is characteristic of corrphycene Mb and is not found in native azide metMb. The EPR in Figure 6 suggests a conformational change or structural heterogeneity of the globin moiety upon sample freezing rather than the freezing out of the spin-state equilibrium. The iron displacement toward N<sub>3</sub><sup>-</sup> in the azide Mb, similar to that found in an azide heme model,<sup>17</sup> weakens the iron-histidine bond to be susceptible to sample freezing. Consistently, the EPR for ferrous corrphycene MbNO at 35 K exhibits a broad signal and sharp three-line hyperfine pattern around  $g = 2$  of comparable magnitude, suggesting mixing of five- and six-coordinate species (result not shown).

**Comparison with Other Azide Proteins.** The azide complexes of native hemoproteins are predominantly low-spin, and the iron-histidine bond is not easily perturbed. Only two examples of the destabilization of the iron-histidine bond are known for the azide complexes of hemoglobin and guanylate cyclase. Perutz et al.<sup>23</sup> indicated that the iron-histidine bond in carp azide hemoglobin is under tension on allosteric transition to the T state. Stone et al.<sup>24</sup> pointed out that azide binding to guanylate cyclase results in high-spin heme, and Makino et al.<sup>25</sup> demonstrated that the iron-histidine bond is broken upon azide binding. The facile bond cleavage in guanylate cyclase suggests

(21) Wu, Y.-D.; Chang, K. W. K.; Yip, C.-P.; Vogel, E.; Plattner, D. A.; Houk, K. N. *J. Org. Chem.* **1997**, *62*, 9240–9250.

(22) Smith, D. W.; Williams, R. J. P. *Biochem. J.* **1968**, *110*, 297–301.

(23) Perutz, M. F.; Sanders, J. K. M.; Chenery, D. H.; Noble, R. W.; Pennelly, R. R.; Fung, L. W.-M.; Ho, C.; Giannini, I.; Pörschke, D.; Winkler, H. *Biochemistry* **1978**, *17*, 3640–3652.

(24) Stone, J. R.; Sands, R. H.; Dunham, W. R.; Maletta, M. A. *Biochemistry* **1996**, *35*, 3258–3262.

(25) Makino, R.; Matsuda, H.; Ohbayashi, E.; Shiro, Y.; Iizuka, T.; Hori, H. *J. Biol. Chem.* **1999**, *274*, 7714–7723.

the possibility that the heme binding cleft imposes constraint on the iron–histidine bond through interactions of protoheme substituents and globin residues. In view of the proximal strain in carp hemoglobin and the azide-induced bond cleavage in guanylate cyclase, the iron–histidine bond in the azide protoheme is only susceptible to the distortion from globin in these oligomeric proteins. On the other hand, the iron–histidine bond in the azide complex of corrphycene-substituted metMb is inherently weak. This interpretation is consistent with the results for the globin-free model compound (Figure 5B), which is predominantly high spin. A close similarity in the IR spectra between the model and protein in Figure 5 further suggests that

the corrphycene in the protein pocket is as flat as the model in organic solvent. In other words, the steric constraint from globin to the corrphycene is insignificant.

It is now clear that rearrangement of the porphyrin skeleton is a promising approach to control the spin equilibrium of hemoprotein. The present work discloses a novel profile of spin equilibrium that could not be foreseen in protoheme enzymes.

**Acknowledgment.** This work was supported by grants-in-aid from the Ministry of Education of Japan (No. 10672031 and Frontier Research Program).

IC000684B